Chemical Engineering & Processing: Process Intensification 217 (2025) 110499

Contents lists available at ScienceDirect

Chemical Engineering and Processing - Process Intensification

journal homepage: www.elsevier.com/locate/cep

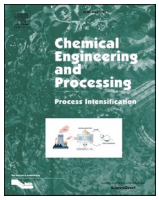

Debottlenecking a 2-phase multi-enzymatic cascade by an enzyme membrane reactor – Modelling and experimental validation

Francesca von Ziegner [a], Grit Brauckmann [b], Volkan Filiz [c], Torsten Brinkmann [c], Paul Bubenheim [b], Thomas Waluga [a,*]

[a] Institute of Process Systems Engineering, Hamburg University of Technology, Germany
[b] Institute of Technical Biocatalysis, Hamburg University of Technology, Germany
[c] Institute of Membrane Research, Helmholtz-Zentrum hereon GmbH, Germany

ARTICLE INFO

Keywords:
Alcohol dehydrogenase
Formate dehydrogenase
Polymeric membranes
Enzyme membrane reactor
Ultrafiltration

ABSTRACT

Biotechnological processes have a high potential to make industrial processes more sustainable. However, biotechnological processes often have low product concentrations and production rates. This is where process intensification can help to make these processes competitive. Using the example of the multi-enzymatic synthesis of natural cinnamyl cinnamate, it is shown how an existing multi-enzymatic process can be intensified by using an enzyme membrane reactor. The individual enzymatic reactions are first characterised in laboratory scale and then combined in a mini plant. In addition, a process model of the mini plant is developed. It is shown that the use of an enzyme membrane reactor can increase the production rate of the multi-enzymatic process by a factor of 10 compared to a previously investigated set-up.

1. Introduction

Biotechnology is undoubtedly one of the most promising scientific fields of our time and is considered to be one of the key technologies of the 21st century [1–4]. It has the potential to make a major contribution to solving global environmental and economic challenges. It enables us to harness living organisms and biological processes for a wide range of applications, from medicine and food production to the manufacture of bioplastics and environmental remediation. As with any breakthrough technology, biotechnology is not without its limitations. One of the key challenges in biotechnology is to intensify these processes to make them more efficient and thus economically competitive with existing chemical processes [5–7]. As biotechnological processes depend on a high number of process parameters, model-based process design is a good tool for designing the best possible process to save time and effort during process synthesis [8]. Therefore, all individual steps in a biotechnological process require a representative mathematical description.

Fragrances and flavourings are typical representatives of biotechnological products, as they can be claimed as 'natural' due to the use of biocatalysts. However, the product concentration of natural flavours and fragrances in biotechnological processes can be very low [9,10]. This study will investigate the kinetic parameters for an enzyme cascade reaction for the reaction of natural flavour cinnamyl cinnamate [11,12]. As first reaction, cinnamyl aldehyde is converted to cinnamyl alcohol by an alcohol dehydrogenase (ADH). As this reaction consumes NADH, a formate dehydrogenase (FDH) is used for cofactor regeneration in a second reaction. These reactions occur in an aqueous phase in the Enzyme Membrane Reactor (EMR). In the following, cinnamyl alcohol is extracted by an organic phase, namely xylene, and is esterified with cinnamic acid by a lipase to form cinnamyl cinnamate, e.g. by the use of a reactive extraction centrifuge (REC) [13]. As enzymes can be very expensive, immobilisation for reuse is a suitable option to increase economics [14,15]. However, the immobilization of ADH and FDH can cause a significant decrease in activity [16] and represent the rate limiting step in this cascade reaction [11]. Therefore, this study is particularly focussing on the process intensification of the reactions in the aqueous phase. To maintain the activity of a native enzyme, a reactor is used where enzymes are restrained by the use of a membrane. The membrane in this case fulfils the purpose of retaining the enzyme and therefore separates the product from the native enzymes by ultrafiltration. The reactants are not separated. The process is operated in a circular flow, which provides a continuous operation of the reactions in the EMR and REC. The overall process scheme is shown in Fig. 1a while Fig. 1b represent the reaction sequence.

* Corresponding author.
E-mail address: thomas.waluga@tuhh.de (T. Waluga).

https://doi.org/10.1016/j.cep.2025.110499
Received 20 February 2025; Received in revised form 15 July 2025; Accepted 7 August 2025
Available online 8 August 2025

This study investigates the temperature dependence of enzymatic reactions using the Arrhenius equation to model the relationship between temperature and reaction kinetics. The temperature dependence of the maximum reaction rate v_{max} will be quantified directly. For the affinity parameters K_M and K_i, which are lumped kinetic constants, their temperature dependence will also be analyzed, although this is more complex and controversially discussed in the literature [17,18]. Therefore, we hypothesis that: the elementary rate constants in enzymatic mechanisms follow the Arrhenius law; if K_M or K_i reflect dissociation constants in rapid equilibrium reactions, they should also exhibit Arrhenius-type behavior [17,18]; if K_M is a composite of multiple rate constants under steady-state conditions, its temperature dependency may be only an apparent effect [18]; and enzyme conformation changes at different temperatures can further affect substrate interactions and thereby influence K_M and K_i [17].

In enzyme kinetics, accurate temperature-dependent parameterization is essential for process design, as both the reaction rate and energy requirements scale with temperature. While higher temperatures typically accelerate reactions, they also increase energy demand and may eventually lead to enzyme denaturation. This study focuses on conditions below the enzyme's denaturation threshold, but if denaturation proves relevant, a multimodel approach might be an alternative [19]. Given the complex and partially unresolved nature of how K_M and K_i, behave with temperature, a purely mechanistic description is very challenging. This work proposes a grey-box modeling approach to describe the temperature dependence of K_M and K_i. This approach allows for practical interpolation of these parameters while acknowledging the theoretical limitations of assigning strict Arrhenius behavior to lumped constants. It provides a flexible yet structured framework for incorporating uncertain or non-elementary temperature effects into kinetic models — a key step toward more robust and economically optimized process design.

2. Materials and methods

In the first section of this chapter, the experiments in lab-scale as well as the mathematical description of the kinetics are explained, which are necessary for the modelling of the process. The second section describes the procedure for model validation, also in lab-scale experiments. In the third section, the final process, according to Fig. 1 is explained in detail.

2.1. Membrane screening

For the screening of the membranes five different polymer membranes were studied at 25 °C. The used membranes consist of poly (octylmethylsiloxane) (POMS), irradiated and not-irradiated poly (dimethylsiloxane) (PDMS), polymers of intrinsic microporosity (PIM), poly(ether-b-amide) (PEBAX®), all coated onto a porous polyacrylonitrile support (PAN). The screening is conducted in a laboratory set-up with three circular membrane modules by Evonik MET, described in detail by Schlüter *et al.* [20]. Each of them is equipped with a membrane cut-out of 14 cm^2. As test conditions a fixed feed flow of 30 Lh^{-1} in order to achieve comparable results and pressures between 0 and 20 bar are used. Within this pressure range a safe operation in the miniplant scale is possible.

The used membranes were of the thin-film-composite type. Detailed information on this type of membrane and how the membrane used in this study are produced can be found in [21]. The composite consists of a non-woven made from polyester on top of which a porous support layer made from polyacrylo nitrile (PAN) is cast. The asymmetric pore structure of the PAN layer is generated by the phase inversion process, described by Scharnagl and Buschatz [22]. The result is in itself a porous micro- or ultrafiltration membrane. The support membrane was produced pilot scale infrastructure at Hereon. It is however available on a commercial basis, e.g. by GMT Membrantechnik GmbH, Rheinfelden,

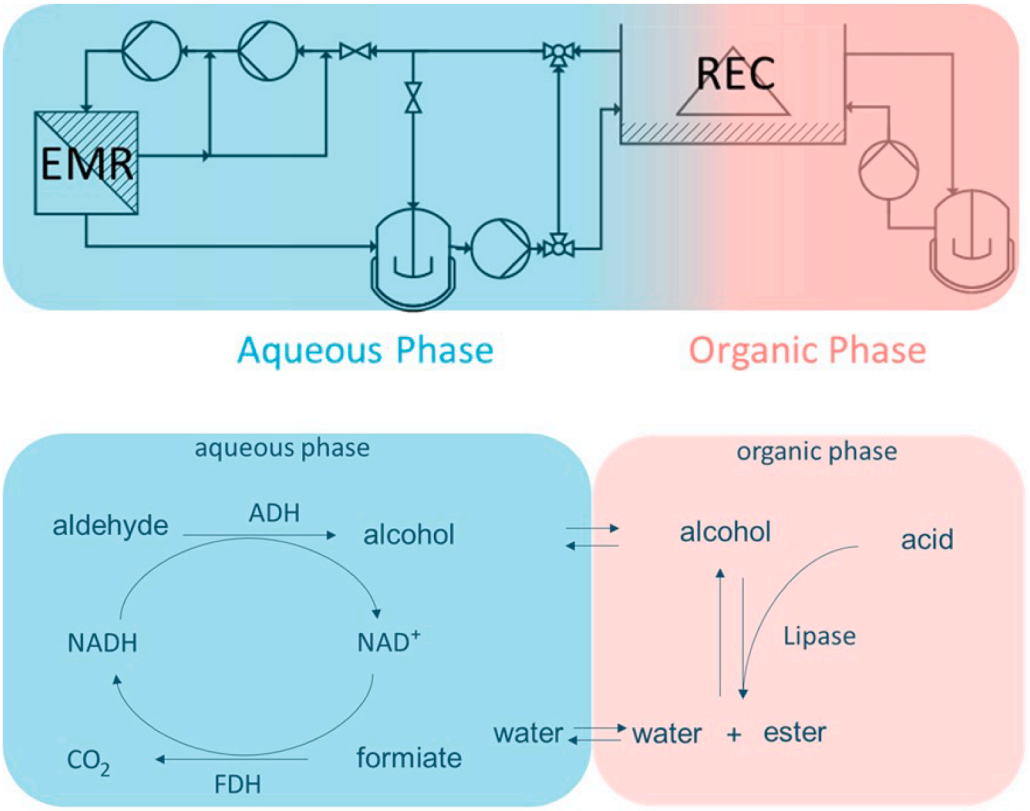

Fig. 1. a) Scheme of the mini plant for the synthesis of cinnamyl cinnamate by a multi-enzymatic cascade. In the aqueous phase with the Enzyme Membrane Reactor (EMR), cinnamyl aldehyde is converted to cinnamyl alcohol by the use of an alcohol dehydrogenase and formate dehydrogenase. In the organic phase the alcohol is esterified with cinnamic acid to form cinnamyl cinnamate in a Reactive Extraction Centrifuge (REC). b) Reaction cascade sequence of the whole process.

Germany. The membranes employed in this study had an additional, dense separation layer. The separation mechanism in this layer adheres to the solution-diffusion mechanism. The layers were applied by a roller coating process, described by Brennecke et al. [23] with subsequent drying and optional cross linking stages. This production was also carried out using Hereon's pilot scale membrane infrastructure. The composite membranes using poly(octylmethylsiloxane) (POMS), irradiated and not-irradiated poly(dimethylsiloxane) (PDMS) as a selective layer are also commercially available via GMT Membrantechnik GmbH, Rheinfelden, Germany. PIM-1 was synthesized by reacting with an equimolar amount of 5,5′,6,6′-tetrahydroxy-3,3,3′,3′-tetramethyl-1, 1′-spirobisindane (TTSBI) and 2,3,5,6-tetrafluoroterephthalo-nitrile (TFTPN) with an excess of K_2CO_3 [24,25]. PEBAX® is a commercially available thermoplastic elastomers poly(ether-block-amide) having flexible polyether and rigid polyamide segments (purchased from Arkema).

2.2. Characterization of the dehydrogenases in lab scale experiment

For the FDH catalyzed reaction progress curves for 20, 30 and 40 °C with different initial substrate concentrations are recorded. The experiments were carried out as a triplet. For formate (Carl Roth GmbH) the initial concentration was 100 mM, 200 mM or 300 mM. NAD^+ (Carl Roth GmbH) was varied in the range of 0.1 mM to 5 mM. A 50 mM phosphate buffer with pH 8.0 was used. FDH from *candida boidinii* (Megazyme Ltd., 75 U mL^{-1}) was diluted to a standard activity of 4 U mL^{-1}. The total reaction volume was 1 mL. The analysis is conducted with UV/VIS spectroscopy at a wave length of 340 nm and a measure interval of 4 s for a maximum of 6 min. This wave length is suitable to determine the NADH concentration, which is one of the products.

For the ADH (Sigma Aldrich GmbH) catalyzed reaction, progress curves with two initial substrate concentrations for 20, 30 and 40 °C were recorded. The experiments were carried out as triplets. The initial concentration of the cinnamyl aldehyde (Sigma Aldrich GmbH) was 0.3 or 1.5 mM, while the NADH (Carl Roth GmbH) concentration was varied over all experiments to be 1 mM, 3 mM or 5 mM. Again a 50 mM phosphate buffer with pH 8.0 was used. 0.35 mg ADH was used. The total reaction volume was 35 mL. Samples were taken every minute for the first 10 min, afterwards every 10 min until a total reaction time of 40 min. The analysis is conducted via gas chromatography with a 0.25 mm × 0.25 µm cross section 30 m SLB SUPELCO® (Supelco, Inc.) column in a Perkin Elmer Clarus 500® gas chromatograph (PerkinElmer Inc.).

2.3. Modelling the temperature dependency of kinetic parameters

In order to determine the temperature dependent kinetic parameters for the ADH and FDH catalyzed reactions, experimental progress curves on a laboratory scale are generated as described above. Both reactions can be described by an irreversible bi-bi mechanism including a product inhibition as described by Eq. (1). It includes the maximal reaction rate v_{max}, the Michaelis-Menten constants K_M and the inhibition constant K_i.

$$v = v_{max} \cdot \frac{[A]\cdot[B]}{K_{m,A}\cdot K_{m,B}\cdot\left(1+\frac{[P]}{K_{i,P}}\right) + K_{m,A}\cdot[B]\cdot\left(1+\frac{[P]}{K_{i,P}}\right) + K_{m,B}\cdot[A] + [A]\cdot[B]} \tag{1}$$

For the FDH catalyzed reaction the substrates A and B are NAD^+ and formate and the inhibiting product P is NADH. For the ADH catalyzed reaction, cinnamyl aldehyde and NADH correspond to substrate A and B and the product cinnamyl alcohol is the inhibitor P.

To describe the temperature dependency the Arrhenius approach [26] is used, cf. Eq. (2).

$$k(T) = k_0 \cdot e^{-\frac{E_A}{R\cdot T}} \tag{2}$$

It is applied for each kinetic parameter individually [27]. Here, k represents the individual kinetic parameter, with k_0 representing the pre-exponential factor, E_A for the activation Energy, R for the universal gas constant and T for the absolute temperature. For the maximum reaction rate this implies the assumption that a higher temperature leads to a higher reaction rate [28]. Furthermore, it is assumed that no thermal deactivation occurs, which should be valid for the studied temperature range between 20 °C till 40 °C [29,30]. The parameter estimation is conducted by using a Matlab script. Spline interpolation is used to smooth and differentiate the experimental progress curves [31]. The concentration dependent reaction rates are fitted to the kinetic equation using *lsqcurvefit*. Here, the lower boundary for all parameters set to 0, while the upper boundary for all parameters were set to *inf*. No further options were applied. The kinetic parameters in Eq. (1) are substituted with temperature dependent parameters in Eq. (2). The fit is conducted with the resulting equation for all temperatures simultaneously [32]. The standard error is calculated manually from the covariance matrix of the parameter estimates, which is obtained by scaling the inverse normal equation matrix with the mean squared deviation.

2.4. Model validation in a lab scale membrane reactor

For the validation of the temperature dependent kinetic parameters and as a proof of concept for the enzyme membrane reactor for this reaction system, further experimental studies on a laboratory scale are conducted and compared with the data from the simulation.

The experimental setup is similar to the membrane screening set up described above. It is operated as a dead-end filtration and the permeate stream is led back into the feed tank. A PEBAX® on PAN membrane is used with a feed flow of 30 L h^{-1}. A temperature of 35 °C is chosen, which is suitable to verify the temperature dependent reaction kinetic and corresponds with the temperature for the operation on miniplant scale. The volume of the three membrane cells with the pipe volumes in between is 0.1 L. Additionally a volume in the feed tank of 0.2 L is required for a continuous operation. The ADH and FDH catalyzed reactions are studied individually. For the FDH reaction, 100 mM formate and 3 mM NAD with 1 mg of FDH were used. For the ADH reaction, 20 mg of enzyme has been used and 2.5 mM cinnamyl aldehyde and 3.3 mM NADH as initial concentration.

For the modeling of the enzyme membrane reactor Python 3.9 is used. The model is implemented as a dynamic model with discrete time steps of one minute. It is assumed that no concentration gradient over the membrane area occurs as the molecular weight cut-off (MWCO) of the membrane allows the substrates and products to pass freely. Further, a dead-end filtration is applied, because of which no retentate flow is considered. The enzyme membrane reactor is considered as a continuously stirred tank membrane reactor (CST-MR). The molar balance for each component i within the enzyme membrane reactor is described as shown in Eq. (3). The reaction rates v_{ADH} and v_{FDH} are considered depending on the stochiometric factor $\upsilon_{i,ADH}$ for each component. The product inhibition for the ADH and FDH catalyzed reaction are considered in the rate equations (Eq. (1)).

$$\frac{dn_{i,\ EMR}}{dt} = \dot{n}_{i,Feed} - \dot{n}_{i,Permeate} + \upsilon_{i,ADH}\cdot v_{ADH} + \upsilon_{i,FDH}\cdot v_{FDH} \tag{3}$$

Similarly, a molar balance for the feed and storage tank is set up as shown in Eq. (4).

$$\frac{dn_{i,\ Tank}}{dt} = \dot{n}_{i,Permeate} - \dot{n}_{i,Feed} \tag{4}$$

Further, a precipitation term is introduced for each component if the solubility concentration of this component is exceeded. It is assumed that this precipitation does not influence the membrane performance. As an autooxidation of NADH to NAD^+ occurs [11], the term in Eq. (5) is added or subtracted to the molar balances, respectively.

$$\frac{dn_{oxidation}}{dt} = [NADH]_{t-1} \cdot (1 - 0.66 \cdot e^{-0.00179}) \quad (5)$$

2.5. Experiments and simulation of the process in a miniplant

The technical realization of the membrane is realized as an envelope type membrane module, described mainly for gas separation processes in literature [33–35]. It allows an individual selection of the membrane area by adding or removing envelopes and flexible application as the membranes can be changed easily compared to spiral wound modules. The mixing was ensured by the usage of spacers between the envelopes. The studied setup consists of a feed tank, three pumps and the enzyme membrane reactor (cf. Fig. 1). It is operated in a cycle. The tank can store a volume of up to 2 L and functions as the feed tank and storage for the permeate flow. With a centrifugal pump the feed stream is pumped from the tank towards the enzyme membrane reactor. Using a piston pump, the pressure is increased to 20 bar. A high flow over the membrane to prevent unwanted accumulation at the membrane is provided by another centrifugal pump. The envelope membrane module has a volume of 1.5 L and a total membrane area of 798 cm^2. The miniplant is operated at a temperature of 35 °C. For model validation the ADH and FDH catalyzed reaction are studied in parallel. Here 43.5 mg of ADH and 7.5 mg of FDH were used. The initial concentration for NADH was 4 mM. As in the context of the whole multi-enzymatic cascade the FDH catalyzed reaction is used to regenerate the produced NAD^+, initially no NAD^+ was added., while no NAD^+ was used as initial condition. 300 mM of formate as initial concentration was set, as well as 8 mM of cinnamyl aldehyde. As the miniplate had been used previously, a residual concentration of 0.5 mM cinnamic alcohol remained despite rinsing. For the simulative study of the miniplant, the enzyme membrane reactor is modeled similar as described in chapter 2.3 with adjusted volumes for the storage tank and the reactor volume. For the comparison with immobilized ADH and FDH on silica beads an already published model and experimental results are used, where also a deactivation coefficient for ADH of 0.7 is considered, as this reaction is running several hours [11].

3. Results and discussion

Following the previous chapter, the first section will present and discuss the experiments in lab-scale for the membrane screening and characterisation of the enzymes. The second section will show the results for the model validation, while in the last section the results of the miniplant are discussed.

3.1. Membrane selection

The membrane selection is conducted based on three criteria: a suitable molecular weight cut-off (MWCO), resistance for the organic solvent xylene and a high permeate flow. As in the enzyme membrane reactor the membrane is required to restrain the enzymes and allow all other components to pass the membrane a MWCO between the size of the ADH or FDH of approximately 41 kDa [36] and 141–151 kDa [37] and the size of next largest component (cinnamyl alcohol) of 134 g • mol^{-1} has to be chosen. As this correlates with size range for ultrafiltration [38], the membranes investigated in this study are suitable for this separation. All of the studied membranes are multilayer composite membranes having a dense separation layer and hence definitely a suitable MWCO. The next screening criterion is the resistance for the organic solvent xylene. As the aqueous phase is constantly in contact with the organic phase and therefore, saturated with xylene, the chosen membrane needs to be xylene-resistant to guarantee a stable operation. For ultrafiltration in the presence of organic solvents polymer membranes rather than inorganic, e.g. ceramic, membranes are used due to their lower production costs and higher flexibility [39]. To test the chemical resistance the polymer membranes screened in this study are stored in xylene for 24 hours. Except for the POMS membrane, no visible changes on the surface were detected. For the POMS membrane a turbidity of the xylene resulting from a detachment of the surface was visible. Therefore, this membrane is not included into the further screening. The third criterion is the permeate flow. Implemented in the process, the permeate flux determines volume flux for the in-situ intermediate removal. Therefore, a high permeate flux is favorable. Fig. 2 shows the results of the membrane screening concerning the permeate flux. The permeate flux is measured over a pressure range of 0 to 20 bar over atmospheric pressure which matches the safety requirements for operation in the laboratory. The PIM membranes, show a low permeate flux over the whole pressure range. The irradiated PDMS and PEBAX® on PAN membranes allow a similar permeate flux of about 30 L • h^{-1} • $m^2_{membrane}$ at 20 bar. As the permeate flux of the PEBAX® on PAN membrane shows a steadier flux between 25 and 32 L • h^{-1} • $m^2_{membrane}$ over the range of 6 to 20 bar, this membrane was chosen to be most suitable for the application in the enzyme membrane reactor for this reaction system.

3.2. Determination of the kinetic parameters

Based on all experiments with FDH the estimated kinetic parameters in respect to Eq. (1) and Eq. (2) are listed in Table 1. A moderate dependence on temperature of the v_{max} and $K_{i,NADH}$ values was detected, where the K_M values show no significant dependency. For the $K_{M,NAD}$ value of FDH from *candida boidinii* the reported values in literature range from 0.015 – 3.4 mM [40,41], depending on individual reaction conditions. For a comparable system a value of 0.04 mM is reported in literature [42], which fits well to the value of 0.053 mM estimated in this study. In literature the value for $K_{M,formate}$ is reported to be much lower [42], however in this study we see a high uncertainty for this value for the fundamental pre-exponential factor. This may be because the applied concentration range could be unsensitive. But the high formate concentration applied in this study is necessary as it ensures a high activity for cofactor regeneration in the whole cascade reaction. For $K_{i,NADH}$ values of 0.020 mM and 0.032 mM have been reported [43], which also fits well to the estimated values of this study, which range from 0.020 mM till 0.029 mM. The estimated v_{max} values of 4.09 till 5.54 U mL^{-1} agree very good with the standard activity, given by the suppliers for a temperature of 25 °C (cf. section 2.1.2).

Fig. 3 shows an example of the good agreement between the experimental data and the model functions at 30 °C obtained using global regression over all temperatures. As can be seen, in experiments with high initial NAD^+ concentrations (1 – 5 mM), the applicable measuring range of the photometer is exceeded after less than 2 min. In contrast, the entire course of the reaction can be measured in experiments with low initial NAD^+ concentrations (0.1 – 0.3 mM). Comparable results are obtained for 20 °C and 40 °C.

For the reaction of ADH, the kinetic parameters listed in Table 2 are obtained. With the exception of $K_{M,aldehyde}$ a moderate temperature dependency can be observed. For the $K_{M,NADH}$ values between 0.025 – 0.177 mM have been reported in literature [44–46], which fits to the rage of the estimated value in this study, which is 0.194 – 0.203 mM. For the reduction of cinnamyl aldehyde the $K_{M,aldehyde}$ values in literature range from 0.01 – 0.39 mM [42], which is at least one order of magnitude below the estimated value in this study, which is 4.147 mM. Unlike $K_{M,formate}$, whose influence is limited due to the high concentration range used, this is not the case for cinnamyl aldehyde. However, as shown in Eq. (1), $K_{M,aldehyde}$ appears only in a term in combination with the inhibition constant $K_{i,alcohol}$. Therefore, an overestimation of $K_{M,aldehyde}$ can be compensated by a corresponding overestimation of $K_{i,alcohol}$. For the $K_{i,alcohol}$ values of 1.3 – 1.6 mM have been estimated, depending on the temperature. In literature, we were not able to identify another $K_{i,alcohol}$ value. However for the reverse reaction a $K_{M,alcohol}$ value for cinnamyl alcohol is reported to be 1.2 mM [47]. If we assume that the product inhibition constant is analogue to the affinity constant

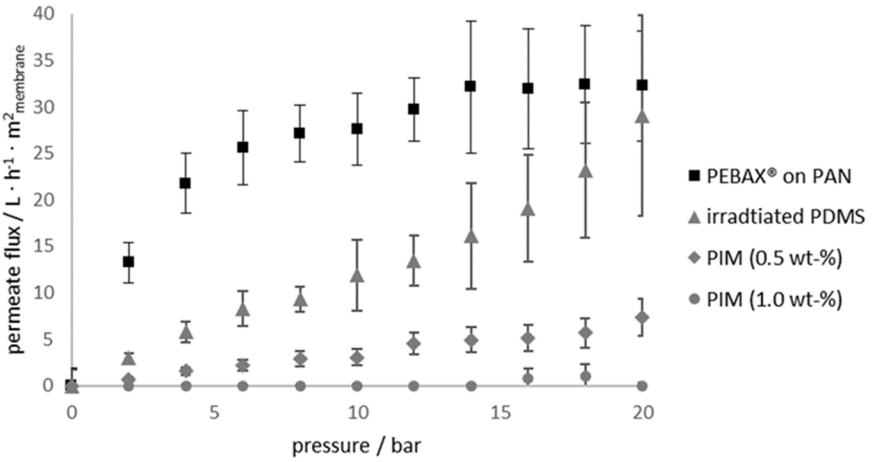

Fig. 2. Results of the membrane screening at 25 °C for four polymer membranes, showing the achieved flux based on different applied pressures. Error bars represents average absolute deviation.

Table 1
Kinetic Data with standard error based on parameter estimation for the FDH reaction based on a holistic parameter estimation from experiments at 20°, 30° and 40 °C in 50 mM phosphate buffer, pH 8.0.

Parameter	pre-exponential factor	Parameter	20 °C	30 °C	40 °C
v_{max0}	484 ± 103 U • mL^{-1}	$\mathbf{v_{max}}$ [U mL^{-1}]	4.09 ± 2.10	4.78 ± 2.41	5.54 ± 2.74
$E_{A0,vmax}$	11,630 ± 541 J • mol^{-1}				
$K_{M0,NAD}$	0.053 ± 0.032 mM	$\mathbf{K_{M,NAD}}$ [mM]	0.053 ± 0.105	0.053 ± 0.102	0.053 ± 0.099
$E_{A0,NAD}$	2 ± 1531 J • mol^{-1}				
$K_{M0,format}$	115 ± 65 mM	$\mathbf{K_{M,format}}$ [mM]	112 ± 205	112 ± 199	112 ± 193
$E_{A0,format}$	59 ± 1432 J • mol^{-1}				
$K_{i0,NADH}$	12.251 ± 11.202 mM	$\mathbf{K_{i,NADH}}$ [mM]	0.020 ± 0.077	0.024 ± 0.092	0.029 ± 0.108
$E_{A0,NADH}$	15,697 ± 2320 • mol^{-1}				

of the reverse reaction, this value can explain partially the overestimation of the Km and is nevertheless itself in the appropriate order of magnitude. For trans-cinnamyl aldehyhde a v_{max} value of 1.1 U mg^{-1} has been reported in literature [48] (where no information on the temperature is given) which is in the same order of magnitude than the estimated values in this study. Overall, the standard errors show that the calculated parameters for the ADH reaction are uncertain, which may be due to an over-parametrization.

Fig. 4 shows an example of the good agreement between the experimental data and the model functions at 30 °C obtained using global regression over all temperatures. Both, the beginning of the reaction with an increased reaction rate as well as the end of the reaction are well reflected by the obtained parameter. Red data represents an experiment with comparably low initial substrate concentrations of 3 mM and 1 mM of NADH and aldehyde, respectively. Blue data represents an experiment with higher initial substrate concentrations of 5 mM and 1.3 mM of NADH and aldehyde, respectively. Comparable results are obtained for 20 °C and 40 °C.

3.3. Results of model validation

The kinetic model parameters for the FDH reaction as well as for the ADH reactions are validated experimentally independently (non-coupled) in a laboratory scale enzyme membrane reactor as described in section 2.2. The kinetic parameters for 35 °C are calculated on the basis of the pre-exponential factors, as they are listed in Table 1 and Table 2. Fig. 5 shows the comparison of simulation data (lines) based on the estimated parameters and experimental data (circles). The left side represents the FDH reaction, while the right side represents ADH reaction.

For the FDH reaction, NADH was measured in the permeate and retentate. As can be seen, there is a very good agreement between experimental und simulated data. For the ADH reaction the cinnamyl aldehyde and the cinnamyl alcohol concentration was measured in the retentate of the membrane. As observed, the experimental and simulated data align very closely for the first 200 min. Subsequently, the reaction rate is slightly overestimated, which is shown by the fact that the experimental cinnamyl aldehyde values are higher than the simulation predictions and the cinnamyl alcohol values are lower than the simulated values. To summarise, it can be stated that the model validation was successful and that the interpolation approach for calculating the parameters at 35 °C also reflects the measured values well.

3.4. Application of an enzyme membrane reactor in a miniplant scale for debottlenecking

In the final set-up the enzymatic reactions are coupled. As described in section 1, ADH is used for the production of cinnamyl alcohol from cinnamyl aldehyde, while FDH provides regenerated cofactor by oxidizing formate. The mixing is ensured by the usage of spacers between the membrane envelopes. The results of the coupled reaction in an enzyme membrane reactor as well as a comparison to previous experiments with enzymes immobilized on silica are shown in Fig. 6. As can be seen, in both experiments a final alcohol yield of approximately 45 % is reached. While this equilibrium is achieved within 5 hours with an Enzyme Membrane Reactor (EMR), the set-up with enzymes immobilized on silica need up to 48 h to reach a comparable concentration. Therefore, the efficiency of the coupled reaction is increased by the factor of approximately 10. This effect is due to the immobilisation of the enzyme in the former setup on silica beads, drastically reducing the activity [16]. An immobilisation can lead to a significant reduction of the remaining activity, leading to a lower reaction rate and therefore longer reaction time. This effect of a reduced activity because of immobilisation is also known from several examples in literature. Bolivar et al. [49] studied the immobilisation of FDH on different carriers with the aim of increasing the stability. This aim was accomplished, but with the drawback of a remaining activity of 15 %. The immobilization of cyclomaltodextrin glucanotransferase enzyme on agarose beads showed a remaining activity of 32 % [50]. Bolivar et al. [51] also investigated the immobilization of ADH, showing a lower activity loss of

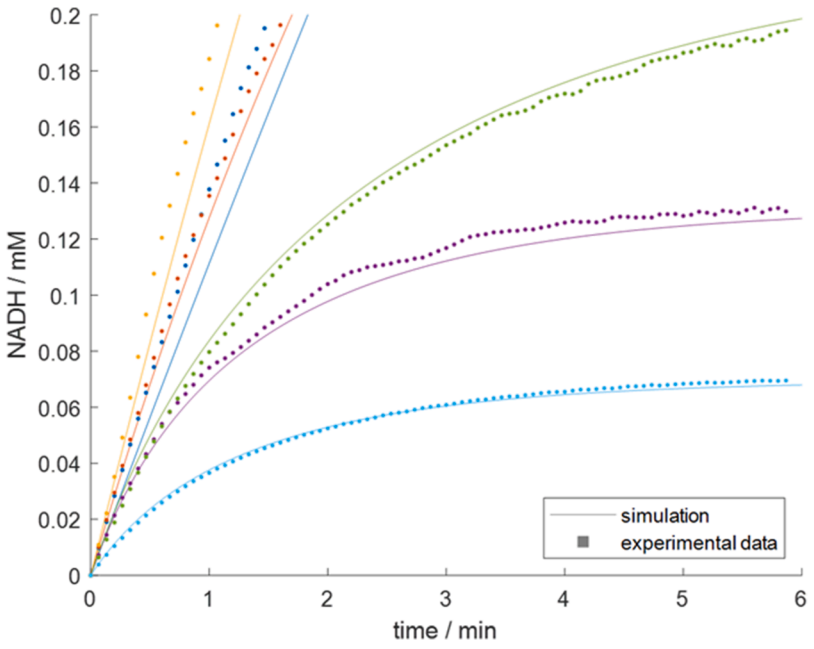

Fig. 3. NADH concentration over time for an FDH reaction at 30 °C with different initial concentration of formate and NAD^+ in a 50 mM phosphate buffer, pH 8.0. Dots represents experimental data based on UV/VIS at 340 nm, solid line represents model function based on experimental data.

Table 2
Kinetic Data for the ADH reaction based on a holistic parameter estimation at 20°, 30° and 40 °C in 50 mM phosphate buffer, pH 8.0.

Parameter	pre-exponential factor	Parameter	20 °C	30 °C	40 °C
v_{max0}	91.850 ± 1654 U • mg-1	$\mathbf{v_{max}}$ [U mL^{-1}]	4.138 ± 1.1 • 10^{10}	4.584 ± 6.3 • 10^{9}	5.044 ± 3.9 • 10^{9}
$E_{A0,vmax}$	7551 ± 45,594 J • mol-1				
$K_{M0,NADH}$	0.385 ± 1.930 mM	$\mathbf{K_{M,NADH}}$ [mM]	0.194 ± 1.7 • 10^{2}	0.199 ± 1.5 • 10^{2}	0.203 ± 1.3 • 10^{2}
$E_{A0,NADH}$	1662 ± 12,222 J • mol^{-1}				
$K_{M0,\ aldehyde}$	4.148 ± 82 mM	$\mathbf{K_{M,aldehyde}}$ [mM]	4.147 ± 8.4 • 10^{10}	4.147 ± 4.2 • 10^{10}	4.147 ± 2.2 • 10^{10}
$E_{A0,\ aldehyde}$	0.125 ± 50,396 J • mol^{-1}				
$K_{i0,alcohol}$	22.833 ± 180 mM	$\mathbf{K_{i,alcohol}}$ [mM]l	1.321 ± 4.4 • 10^{4}	1.451 ± 3.7 • 10^{4}	1.585 ± 3.1 • 10^{4}
$E_{A0,alcool}$	6942 ± 20,050 J • mol^{-1}				

10 % compared to the other examples.

The simulation of the EMR show a good agreement between experimental and simulated data. The simulation shows systematically a slight overestimation of the concentration. This may be due to undefined interactions of the enzymes with each other or with the non native reactants, as our models only consider product inhibition but no reverse reaction or other inhibitions. Based on the BRENDA – The Comprehensive Enzyme Information System database [52], for ADH there is no interaction with formate reported and for the FDH there is no interaction with a cinnamyl reactant reported. However, this is not an exclusion criterion, but merely indicates that such interactions might not have been investigated yet. In general, the time course of the reaction in this study is represented well and the interpolation of temperature dependency is described satisfactorily.

4. Summary and outlook

In this work, an enzyme membrane reactor was successfully used to retain the enzyme, as an alternative to enzyme immobilization on solid silica particle, to intensify a co-factor coupled reaction. Initially, a suitable membrane, with a PEBAX® separation layer on a PAN porous support, was identified, which met the requirements of enzyme retention, chemical stability against all used chemicals, and high flux. The individual enzymatic reactions were carried out at different temperatures in lab scale experiments, and the kinetic parameters were modelled as a function of temperature. The validation of the parameters was conducted in a lab scale membrane reactor. For model validation, a temperature was chosen at which the experimental characterization had not been conducted. It was ensured that only interpolation occurred, as unpredictable interactions may arise outside the measurement range. For the validation, the reactions were conducted individually. The estimated kinetic parameters for the two reactions could be validated well by experimental values. Finally, the coupled reaction was conducted in a miniplant and the measured data were compared with the developed models and with previous experimental data achieved with immobilized enzymes. Here, a good agreement between experimental data and the model was achieved. Additionally, it was demonstrated that using a membrane reactor and native enzymes could intensify the coupled reaction and reduce the reaction time by a factor of 10.

The study presented herein constitutes a segment of a more intricate multi-enzyme cascade operating within a biphasic system. Future research efforts will focus on the experimental realization of the complete process. In this regard, the developed models offer a valuable contribution for the preliminary determination of optimal operating parameters and serve as a foundation for systematic process optimization.

Data statement

Experimental data are available at TORE (TUHH Open Research) https://doi.org/10.15480/882.14605.

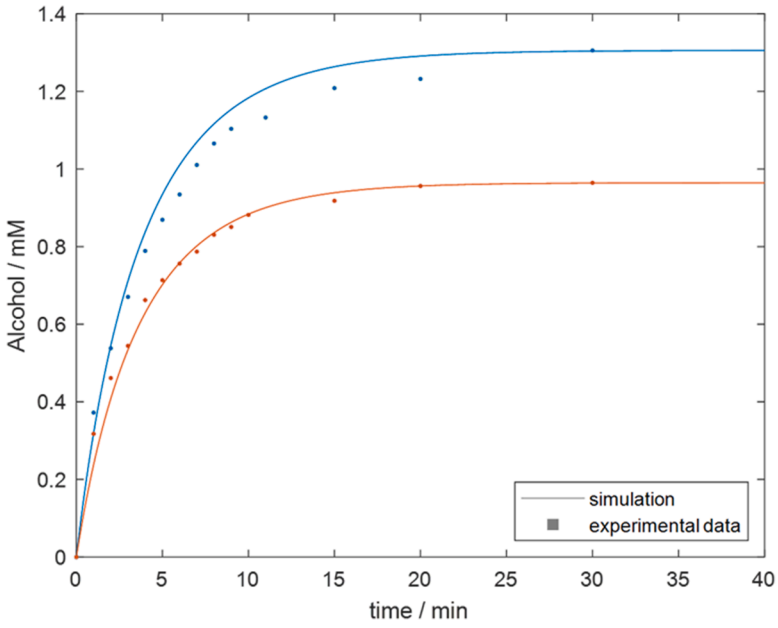

Fig. 4. Cinnamyl alcohol concentration over time for an AHD reaction at 30 °C with different initial concentration of cinnamyl alcohol and NADH in a 50 mM phosphate buffer, pH 8.0. Initial concentration of NADH 5 mM and aldehyde 1.3 mM (blue), respectively NADH 3 mM and aldehyde 1 mM (red). Dots represents experimental data, solid line represents model function based on experimental data.

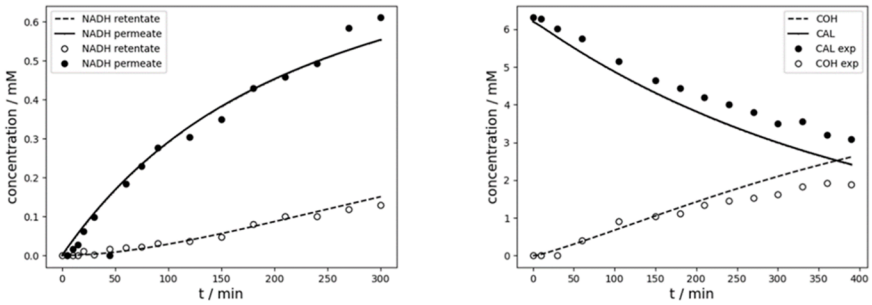

Fig. 5. Experimental data and simulation of the membrane reactor. Left: NADH concentration over time for an FDH reaction at 35 °C, 50 mM phosphate buffer, pH 8.0. Right: Cinnamyl alcohol (COH) and cinnamyl aldehyde (CAL) concentration over time for an ADH reaction at 35 °C, 50 mM phosphate buffer, pH 8.0. Initial concentrations are described in section 2.2.

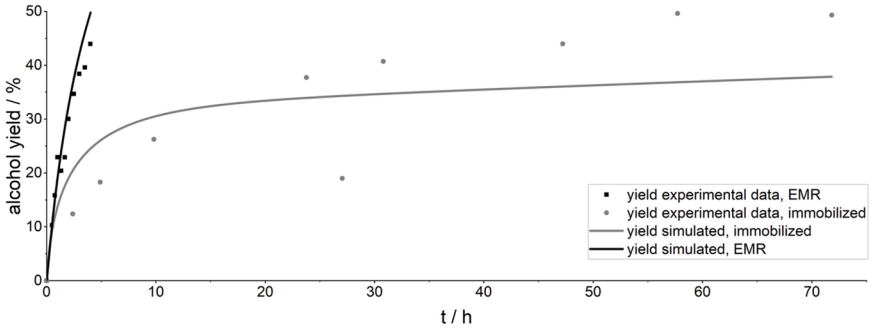

Fig. 6. Experimental data and simulation of the mini plant. Black coloured data for this study with a membrane for immibilization. Grey coloured data for immobilized set-up taken from [11].

Funding details

This work was supported by the German Research Foundation [project number 321884682] and co-funded by an I^3 Junior Project of Hamburg University of Technology.

CRediT authorship contribution statement

Francesca von Ziegner: Writing – review & editing, Visualization, Validation, Software, Methodology, Investigation, Funding acquisition, Formal analysis, Data curation, Conceptualization. **Grit Brauckmann:** Writing – review & editing, Methodology, Investigation, Funding

acquisition. **Volkan Filiz:** Writing – review & editing, Resources, Conceptualization. **Torsten Brinkmann:** Writing – review & editing, Resources, Conceptualization. **Paul Bubenheim:** Writing – review & editing, Supervision, Project administration, Funding acquisition. **Thomas Waluga:** Writing – review & editing, Writing – original draft, Visualization, Validation, Supervision, Software, Project administration, Methodology, Funding acquisition, Formal analysis, Data curation, Conceptualization.

Declaration of competing interest

The authors report there are no competing interests to declare.

Data availability

I have share the link to my data in the manuscript.

References

[1] acatech – National Academy of Science and Engineering, Innovation Potential of Biotechnology, acatech IMPULSE, 2017. Available online, https://en.acatech.de/publication/innovation-potential-of-biotechnology/. accessed on 19 August 2024.

[2] Presse- und Informationsamt der Bundesregierung. *Zukunftsrat des Bundeskanzlers sieht in der Biotechnologie eine Schlüsseltechnologie für den Standort Deutschland: pressemitteilung 146;* Berlin, 2023.

[3] U.S. Economic Development Administration. *Biden-harris administration designates tech hub in Alabama to increase representation in clinical data and improve pharmaceutical development: as part of the president's investing in America agenda, the U.S. department of commerce identifies regional centers primed for innovation and job creation.*, 2023.

[4] K. Boodhoo, M.C. Flickinger, J.M. Woodley, E. Emanuelsson, Bioprocess intensification: a route to efficient and sustainable biocatalytic transformations for the future, Chem. Eng. Process. - Process Intensif. 172 (2022) 108793, https://doi.org/10.1016/j.cep.2022.108793.

[5] J.M. Woodley, Accelerating the implementation of biocatalysis in industry, Appl. Microbiol. Biotechnol. 103 (2019) 4733–4739, https://doi.org/10.1007/s00253-019-09796-x.

[6] F.-D. Vivien, M. Nieddu, N. Befort, R. Debref, M. Giampietro, The Hijacking of the Bioeconomy, Ecol. Econ. 159 (2019) 189–197, https://doi.org/10.1016/j.ecolecon.2019.01.027.

[7] F. Paradisi, Stepping up: from lab scale to industrial processes, Chem. Eng. Process. - Process Intensif. 208 (2025) 110094, https://doi.org/10.1016/j.cep.2024.110094.

[8] Y. Sewsynker-Sukai, F. Faloye, E.B.G. Kana, Artificial neural networks: an efficient tool for modelling and optimization of biofuel production (a mini review), Biotechnol. Biotechnol. Equip. 31 (2017) 221–235, https://doi.org/10.1080/13102818.2016.1269616.

[9] N.J. Gallage, E.H. Hansen, R. Kannangara, C.E. Olsen, M.S. Motawia, K. Jørgensen, I. Holme, K. Hebelstrup, M. Grisoni, B.L. Møller, Vanillin formation from ferulic acid in Vanilla planifolia is catalysed by a single enzyme, Nat. Commun. 5 (2014) 4037, https://doi.org/10.1038/ncomms5037.

[10] A.K. Sinha, U.K. Sharma, N. Sharma, A comprehensive review on vanilla flavor: extraction, isolation and quantification of vanillin and others constituents, Int. J. Food Sci. Nutr. 59 (2008) 299–326, https://doi.org/10.1080/09687630701539350.

[11] J. Johannsen, F. Meyer, C. Engelmann, A. Liese, G. Fieg, P. Bubenheim, T. Waluga, Multi-enzyme cascade reaction in a miniplant two-phase-system: model validation and mathematical optimization, AIChE J. 67 (2021), https://doi.org/10.1002/aic.17158.

[12] F. Meyer, J. Johannsen, A. Liese, G. Fieg, P. Bubenheim, T. Waluga, Evaluation of process integration for the intensification of a biotechnological process, Chem. Eng. Process. - Process Intensif. 167 (2021) 108506, https://doi.org/10.1016/j.cep.2021.108506.

[13] F. Meyer, N. Gasimov, P. Bubenheim, T. Waluga, Concept of an Enzymatic Reactive Extraction Centrifuge, Processes 10 (2022) 2137, https://doi.org/10.3390/pr10102137.

[14] F. Liu, Z. Shi, W. Su, J. Wu, State of the art and applications in nanostructured biocatalysis, Biotechnol. Biotechnol. Equip. 36 (2022) 118–134, https://doi.org/10.1080/13102818.2022.2054727.

[15] N.R. Mohamad, N.H.C. Marzuki, N.A. Buang, F. Huyop, R.A. Wahab, An overview of technologies for immobilization of enzymes and surface analysis techniques for immobilized enzymes, Biotechnol. Biotechnol. Equip. 29 (2015) 205–220, https://doi.org/10.1080/13102818.2015.1008192.

[16] C. Engelmann, N. Ekambaram, J. Johannsen, O. Fellechner, T. Waluga, G. Fieg, A. Liese, P. Bubenheim, Enzyme immobilization on synthesized nanoporous silica particles and their application in a bi-enzymatic reaction, ChemCatChem. 12 (2020) 2245–2252, https://doi.org/10.1002/cctc.201902293.

[17] A. Cornish-Bowden, *Fundamentals of Enzyme Kinetics*, 4th, Completely rev. and Greatly Enlarged ed., 1st Corrected Reprint, Wiley-Blackwell, Weinheim, Germany, 2012, 2014ISBN 9783527330744.

[18] I.H. Segel, *Enzyme Kinetics: Behavior and Analysis of Rapid Equilibrium and Steady-State Enzyme Systems*, John Wiley & Sons, New York, 2014 dr.ISBN 9780471303091.

[19] T. Pencheva, S. Vassileva, T. Ilkova, Y. Georgieva, B. Hitzmann, S. Tzonkov, Multimodel approach for modelling of biotechnological processes, Biotechnol. Biotechnol. Equip. 18 (2004) 206–214, https://doi.org/10.1080/13102818.2004.10817112.

[20] S. Schlüter, K.U. Künnemann, M. Freis, T. Roth, D. Vogt, J.M. Dreimann, M. Skiborowski, Continuous co-product separation by organic solvent nanofiltration for the hydroaminomethylation in a thermomorphic multiphase system, Chem. Eng. J. 409 (2021) 128219, https://doi.org/10.1016/j.cej.2020.128219.

[21] V. Abetz, T. Brinkmann, M. Dijkstra, K. Ebert, D. Fritsch, K. Ohlrogge, D. Paul, K.-V. Peinemann, S. Pereira-Nunes, N. Scharnagl, et al., Developments in membrane research: from material via process design to industrial application, Adv. Eng. Mater. 8 (2006) 328–358, https://doi.org/10.1002/adem.200600032.

[22] N. Scharnagl, H. Buschatz, Polyacrylonitrile (PAN) membranes for ultra- and microfiltration, Desalination. 139 (2001) 191–198, https://doi.org/10.1016/S0011-9164(01)00310-1.

[23] F. Brennecke, J. Clodt, J. Pohlmann, C. Abetz, T. Brinkmann, V. Abetz, Computational fluid dynamics simulation of the roll-to-roll coating process for the production of thin film composite membranes including validation, J. Adv. Manuf. Process. 3 (2021), https://doi.org/10.1002/amp2.10076.

[24] T. Koschine, K. Rätzke, F. Faupel, M.M. Khan, T. Emmler, V. Filiz, V. Abetz, L. Ravelli, W. Egger, Correlation of gas permeation and free volume in new and used high free volume thin film composite membranes, J. Polym. Sci. B Polym. Phys. 53 (2015) 213–217, https://doi.org/10.1002/polb.23616.

[25] M.M. Khan, G. Bengtson, S. Shishatskiy, B.N. Gacal, M. Mushfequr Rahman, S. Neumann, V. Filiz, V. Abetz, Cross-linking of Polymer of Intrinsic Microporosity (PIM-1) via nitrene reaction and its effect on gas transport property, Eur. Polym. J. 49 (2013) 4157–4166, https://doi.org/10.1016/j.eurpolymj.2013.09.022.

[26] G.G. Stavropoulos, M. Papadopoulou, K. Papadimitriou, A kinetic and thermodynamic study of cyanide adsorption in activated carbon, Desalin. Water Treat 57 (2016) 21939–21943, https://doi.org/10.1080/19443994.2015.1127777.

[27] A.M. Dehkordi, M.S. Tehrany, I. Safari, Kinetics of glucose isomerization to fructose by immobilized glucose isomerase (Sweetzyme IT), Ind. Eng. Chem. Res. 48 (2009) 3271–3278, https://doi.org/10.1021/ie800400b.

[28] V.L. Arcus, A.J. Mulholland, Temperature, dynamics, and enzyme-catalyzed reaction rates, Annu. Rev. Biophys. 49 (2020) 163–180, https://doi.org/10.1146/annurev-biophys-121219-081520.

[29] Y. Yang, R. Chen, H.M. Zhou, Comparison of inactivation and conformational changes of native and apo yeast alcohol dehydrogenase during thermal denaturation, Biochem. Mol. Biol. Int. 45 (1998) 475–487, https://doi.org/10.1080/15216549800202862.

[30] G. Pietricola, T. Tommasi, M. Dosa, E. Camelin, E. Berruto, C. Ottone, D. Fino, V. Cauda, M. Piumetti, Synthesis and characterization of ordered mesoporous silicas for the immobilization of formate dehydrogenase (FDH), Int. J. Biol. Macromol. 177 (2021) 261–270, https://doi.org/10.1016/j.ijbiomac.2021.02.114.

[31] T. Waluga, F. von Ziegner, M. Skiborowski, Analytical and numerical approaches to the analysis of progress curves: a methodological comparison, Process Biochem. 151 (2025) 1–13, https://doi.org/10.1016/j.procbio.2025.01.029.

[32] M. Porcel, J. Staudt, G. Spohr, C. Da Silva, C. Borba, Effect of the Temperature and Molar Ratio of Water-Oil on the Enzymatic Hydrolysis Kinetics of the Soybean Oil: experimental and Mathematical Modeling, J. Braz. Chem. Soc. (2023), https://doi.org/10.21577/0103-5053.20230061.

[33] T. Brinkmann, C. Naderipour, J. Pohlmann, J. Wind, T. Wolff, E. Esche, D. Müller, G. Wozny, B. Hoting, Pilot scale investigations of the removal of carbon dioxide from hydrocarbon gas streams using poly (ethylene oxide)–poly (butylene terephthalate) PolyActive™) thin film composite membranes, J. Memb. Sci. 489 (2015) 237–247, https://doi.org/10.1016/j.memsci.2015.03.082.

[34] T. Brinkmann, J. Pohlmann, M. Bram, L. Zhao, A. Tota, N. Jordan Escalona, M. de Graaff, D. Stolten, Investigating the influence of the pressure distribution in a membrane module on the cascaded membrane system for post-combustion capture, Int. J. Greenh. Gas Control. 39 (2015) 194–204, https://doi.org/10.1016/j.ijggc.2015.03.010.

[35] T. Brinkmann, J. Pohlmann, U. Withalm, J. Wind, T. Wolff, Theoretical and Experimental Investigations of Flat Sheet Membrane Module Types for High Capacity Gas Separation Applications, Chem. Ing. Tech. 85 (2013) 1210–1220, https://doi.org/10.1002/cite.201200238.

[36] Megazyme Ltd. *Datasheet formate dehydrogenase*. Available online: https://d1kkimny8vk5e2.cloudfront.net/documents/Data_Sheet/E-FDHCB_DATA.pdf (accessed on 29 November 2024).

[37] Sigma-Aldrich Co. LLC. *Datasheet alcohol dehydrogenase*. Available online: https://www.sigmaaldrich.com/deepweb/assets/sigmaaldrich/product/documents/213/220/a7011dat.pdf (accessed on 29 November 2024).

[38] W.J. Koros, Y.H. Ma, T. Shimidzu, Terminology for membranes and membrane processes (IUPAC Recommendations 1996), Pure Appl. Chem. 68 (1996) 1479–1489, https://doi.org/10.1351/pac199668071479.

[39] C.M. Sánchez-Arévalo, M.C. Vincent-Vela, M.-J. Luján-Facundo, S. Álvarez-Blanco, Ultrafiltration with organic solvents: a review on achieved results, membrane materials and challenges to face, Process Saf. Environ. Prot. 177 (2023) 118–137, https://doi.org/10.1016/j.psep.2023.06.073.

[40] A. Andreadeli, D. Platis, V. Tishkov, V. Popov, N.E. Labrou, Structure-guided alteration of coenzyme specificity of formate dehydrogenase by saturation

mutagenesis to enable efficient utilization of NADP+, FEBS. J. 275 (2008) 3859–3869, https://doi.org/10.1111/j.1742-4658.2008.06533.x.
[41] W. Jiang, P. Lin, R. Yang, B. Fang, Identification of catalysis, substrate, and coenzyme binding sites and improvement catalytic efficiency of formate dehydrogenase from Candida boidinii, Appl. Microbiol. Biotechnol. 100 (2016) 8425–8437, https://doi.org/10.1007/s00253-016-7613-6.
[42] C. Engelmann, J. Johannsen, T. Waluga, G. Fieg, A. Liese, P. Bubenheim, A multi-enzyme cascade for the production of high-value aromatic compounds, Catalysts. 10 (2020) 1216, https://doi.org/10.3390/catal10101216.
[43] N. Kato, H. Sahm, F. Wagner, Steady-state kinetics of formaldehyde dehydrogenase and formate dehydrogenase from a methanol-utilizing yeast, Candida boidinii, Biochim. Biophys. Acta 566 (1979) 12–20, https://doi.org/10.1016/0005-2744(79)90243-2.
[44] M. Vitolo, E. Junko Yoriyaz, Reduction of prochiralic ketones by NAD(H)-dependent alcohol dehydrogenase in membrane reactor, AJS 2 (2015) 161–176, https://doi.org/10.30958/ajs.2-3-1.
[45] F. Marpani, Z. Sárossy, M. Pinelo, A.S. Meyer, Kinetics based reaction optimization of enzyme catalyzed reduction of formaldehyde to methanol with synchronous cofactor regeneration, Biotechnol. Bioeng. 114 (2017) 2762–2770, https://doi.org/10.1002/bit.26405.
[46] C. Drewke, M. Ciriacy, Overexpression, purification and properties of alcohol dehydrogenase IV from Saccharomyces cerevisiae, Biochim. Biophys. Acta 950 (1988) 54–60, https://doi.org/10.1016/0167-4781(88)90072-3.
[47] R. Pietruszko, K. Crawford, D. Lester, Comparison of substrate specificity of alcohol dehydrogenases from human liver, horse liver, and yeast towards saturated and 2-enoic alcohols and aldehydes, Arch. Biochem. Biophys. 159 (1973) 50–60, https://doi.org/10.1016/0003-9861(73)90428-1.
[48] A.M. Klibanov, P.P. Giannousis, Geometric specificity of alcohol dehydrogenases and its potential for separation of trans and cis isomers of unsaturated aldehydes, Proc. Natl. Acad. Sci. U. S. A 79 (1982) 3462–3465, https://doi.org/10.1073/pnas.79.11.3462.
[49] J.M. Bolivar, L. Wilson, S.A. Ferrarotti, R. Fernandez-Lafuente, J.M. Guisan, C. Mateo, Evaluation of different immobilization strategies to prepare an industrial biocatalyst of formate dehydrogenase from Candida boidinii, Enzyme Microb. Technol. 40 (2007) 540–546, https://doi.org/10.1016/j.enzmictec.2006.05.009.
[50] P.W. Tardioli, G.M. Zanin, F.F.de Moraes, Characterization of Thermoanaerobacter cyclomaltodextrin glucanotransferase immobilized on glyoxyl-agarose, Enzyme Microb. Technol. 39 (2006) 1270–1278, https://doi.org/10.1016/j.enzmictec.2006.03.011.
[51] J.M. Bolivar, L. Wilson, S.A. Ferrarotti, J.M. Guisán, R. Fernández-Lafuente, C. Mateo, Improvement of the stability of alcohol dehydrogenase by covalent immobilization on glyoxyl-agarose, J. Biotechnol. 125 (2006) 85–94, https://doi.org/10.1016/j.jbiotec.2006.01.028.
[52] A. Chang, L. Jeske, S. Ulbrich, J. Hofmann, J. Koblitz, I. Schomburg, M. Neumann-Schaal, D. Jahn, D. Schomburg, BRENDA, the ELIXIR core data resource in 2021: new developments and updates, Nucleic. Acids. Res. 49 (2021) D498–D508, https://doi.org/10.1093/nar/gkaa1025.